

Working Title:

A thermodynamic model describing the nature of the crista junction; a structural motif in the mitochondrion.

Christian Renken†\*, Gino Siragusa‡, Guy Perkins§, Lance Washington†, Jim Nulton‡, Peter Salamon‡, and Terrence G. Frey†§.

†Department of Biology San Diego State University, San Diego, CA 92185

‡Department of Physics San Diego State University, San Diego, CA 92185

§National Center for Microscopy and Imaging Research, University of California San Diego, La Jolla, CA

**Key Words:** electron tomography, membrane topology, mitochondria, modeling, spontaneous curvature.

\*To whom correspondence should be addressed:

Christian Renken

Wadsworth Center, NY State Dept. Health

Empire State Plaza, P.O.Box 509

Albany, NY 12201-0509

Tel: 518-473-0202

Fax: 518-474-7992

Email:renken@wadsworth.org

**Abstract:** The use of electron tomography has allowed the three-dimensional membrane topography of the mitochondrion to be better understood. The most striking feature of this topology is the crista junction, a structure that may serve to divide functionally the inner-membrane and inter-membrane spaces. In situ these junctions seem to have a preferred size and shape independent of the source of the mitochondrion with few exceptions. When mitochondria are isolated and have a condensed matrix the crista junctions enlarge and become non-discrete. Upon permeation of the inner membrane and subsequent swelling of the matrix space, the uniform circular nature of the crista junction reappears. We examine the distribution of shapes and sizes of crista junctions and suggest a thermodynamic model that explains the distribution based on current theories of bilayer membrane shapes. The theory of spontaneous curvature shows the circular junction to be a thermodynamically stable structure whose size and shape is influenced by the relative volume of the matrix. We conclude that the crista junction exists predominantly as a circular junction with other shapes as exceptions made possible by specific characteristics of the lipid bilayer.

## Introduction:

The use of tomography to look at the structure of the mitochondria revealed a structural motif known as the crista junction (Perkins *et al* 1997; Mannella *et al* 1994; Frey and Mannella 2000). This structural motif was suggested earlier by Daems and Wisse (Daems and Wisse 1966), but was not widely accepted. One reason may be that in isolated mitochondria this structural motif is not always present; isolated liver mitochondria contain crista junctions (Mannella *et al* 1994), but isolated *Xenopus* mitochondria have a more highly condensed matrix and contain large irregularly shaped junctions (figures 1b,2b) (Kluck *et al* 1999; von Ahsen *et al* 2000). In experiments looking at possible mechanisms of cytochrome c release, *Xenopus* mitochondria were purposely treated to permeate the inner membrane and swell the matrix, causing the crista junction motif to reappear (von Ahsen *et al* 2000) (figures 1c,2b).

These results suggest that the crista junction motif may be a result of the folding properties of the inner membrane. Orthodox mitochondria (Hackenbrock 1966) are characterized by an expanded matrix forcing the periphery of the inner membrane into close apposition with the outer membrane and the transition from inner boundary membrane to crista membrane forms a ninety-degree bend in the membrane. Bending a lipid bilayer requires finite amounts of energy and the size of the junction determines the amount of bilayer bend. The focus of this investigation was initiated by the observation that an exponential distribution of the form

$$e^{-\left(\frac{a}{x^m} + bx\right)} \quad (1)$$

fit the observed distribution of crista junction diameters better than a normal distribution, as measured by a chi-squared goodness of fit (see figure 2d below). Condensed

mitochondria show two morphologies. Some have inflated cristae and retain the crista junction morphology (Mannella *et al* 1994), whereas in others, the periphery of the inner membrane was pulled away from the outer membrane and the uniform nature of the crista junction was lost. (von Ahsen *et al* 2000). In these mitochondria there does not exist the high degree of bending associated with the crista junction, due to the pulling away of the inner boundary membrane, and thus the influence of bending energy is lessened.

### *Spontaneous Curvature Theory Of Lipid Vesicle Shape*

A large body of literature exists attempting to predict the shape of lipid vesicles (Lipowsky 1991). Beginning with Canham (Canham 1970) and followed by Helfrich (Helfrich 1973) membrane curvature was treated as a perturbation from equilibrium, defined as a flat surface (Canham) or surface with spontaneous curvature  $C_0$  (Helfrich). Helfrich derived the spontaneous curvature energy model based on elastic curvature theory in liquid crystals (Jie *et al* 1998). He proposed that, to lowest order, the energy density due to bending was a quadratic function of the two principal curvatures and a spontaneous curvature, which accounted for differences between the two sheets of the lipid bilayer. Given a surface with principal curvatures  $C_1$  and  $C_2$  and a spontaneous curvature  $C_0$  the energy due to membrane bending is

$$E_b = K_b \iint \left( \frac{C_1 + C_2}{2} - C_0 \right)^2 dA + \iint k_g C_1 C_2 dA \quad (2)$$

The Gaussian curvature term, the second integral, is constant for constant topology and can be neglected when considering the morphology of the crista junctions. The bending rigidity  $K_b$  is a property of the molecular make up of the lipid bilayer depending on

temperature, lipid content, and protein content. The free energy for a closed lipid vesicle is given by

$$F = E_b + \Delta p \int dV + \lambda \oint dA . \quad (3)$$

The second and third integrals account for osmotic pressure and stretching respectively. Minimization of equation 2 has been extensively explored for the modeling of vesicle shapes for given volume and stretch (Naito *et al* 1995; Lipowsky 1991; Zhong-can and Helfrich 1987; Zhong-can and Helfrich 1989).

This paper examines observations of mitochondrial geometry in the vicinity of crista junctions. We compare these observations with calculations of the bending energy in these junctions. We find that our observations of the distribution of crista junction radii conform to that predicted by an energetic distribution determined by curvature energy. Fitting parameters give a bending energy modulus  $K_b$  and spontaneous curvature  $C_0$  consistent with those previously published (Goetz and Gompper 1998; Jung *et al* 2001). We then assume that crista junctions are a result of minimizing the curvature energy and use the surface modeling program SURFACE EVOLVER to elucidate a possible mechanism of crista generation. We find that the spontaneous curvature theory; (1) explains the homogeneity of crista junctions, exceptions like elliptical junctions, and their change in shape due to changes in matrix volume; and (2) allows for a simple mechanism of crista formation.

## MATERIAL AND METHODS

### *Electron Tomography:*

Tomograms of mitochondria were taken from a variety of experiments described elsewhere (Lutter *et al* 2002; Perkins *et al* 1998; Kluck *et al* 1999; Perkins *et al* 1997; Perkins *et al* 2001; Perkins *et al* 2001). Generally a tilt series is acquired from  $-60$  degrees to  $+60$  degrees in 2 degree increments on a JOEL 4000EX microscope operating at 400kv. Images were aligned by a least-squares fit of picked fiducial marks. Reconstruction was by the R-weighted back-projection algorithm.

### *Measurements and Analysis:*

Volumes were then either analyzed in NIH Image (Macintosh) or ImageJ (PC) (<http://rsb.info.nih.gov/nih-image/about.html>) to measure the radius ( $R$ ) and flare ( $r$ ) of observed crista junctions. For each crista junction  $R$  and  $r$  were measured in the z-slice that represented the center of the crista junction.  $R$  was measured by half the distance from midpoint to mid point of the crista membranes at the top of the junction. We estimated  $r$  by fitting a quarter circle to each side of the junction and taking the average. A ratio of radii ( $R'$ ) for each junction was then calculated as  $R/r$ . The values of the  $R$ ,  $R'$ , and  $r$  were grouped according to source, and then tested by analysis of variance (ANOVA) for significance of differences in mean values. Rejection of the hypothesis was made at the .01 level by student's t-test.

### *Modeling:*

Surface rendered models of mitochondria were made by segmenting the membranes in XVOXTRACE (<http://ncmir.ucsd.edu/sp.html#voxtrace>) and then converting the contours to surfaces using nuages. Surfaces were then visualized and rendered in SYNUIVIEW (<http://ncmir.ucsd.edu/sp.html#synu>) (Hessler *et al* 1992).

Formation of crista and crista junctions were modeled by the surface modeling program SURFACE EVOLVER (<http://www.susqu.edu/brakke/evolver/evolver.html>). SURFACE EVOLVER (Brakke 1992; Zhou *et al* 2002) triangulates a surface by calculating the energy around discrete points on the surface. The user has control over which energies will be included and can also define new energies. Given a target volume and surface area the program will then evolve a surface that minimizes the summed energies.

Models of theoretical crista junctions and derivations of bending energy were made using the program MAPLE (<http://www.maplesoft.com/flash/index.html>).

### *Analysis Of Crista Junctions*

Based upon our observations of crista junctions we modeled an ideal crista junction with the following parametric surface  $(x(u,v), y(u,v), z(u,v))$ .

$$x = r\left(\frac{R}{r} + 1 - \cos(u)\right)\cos(v), \quad y = r\left(\frac{R}{r} + 1 - \cos(u)\right)\sin(v), \quad z = r(1 - \sin(u)) \quad (4)$$

Equation four describes the bell of a trumpet with  $r$  as the radius of curvature of the flare of the trumpet and  $R$  as the radius of the opening (figure 1d). This model satisfied three conditions: (1) the boundary conditions of having a vertical surface at  $R$  and a horizontal surface at  $R + r$ ; (2) the controlling parameters  $R$  and  $r$  could be measured by the programs NIH Image or Image J; and (3) gave analytical solutions to the left integral in

equation 2. Substituting  $R' = \frac{R}{r}$  and using differential geometry and MAPLE

([http://www.mapleapps.com/categories/mathematics/differential\\_geometry/html/surbasic.html](http://www.mapleapps.com/categories/mathematics/differential_geometry/html/surbasic.html)) to calculate the mean curvature of the surface gives

$$\frac{C_1 + C_2}{2} = -\frac{1}{2} \frac{2 \cos(u) - R' - 1}{r(\cos(u) - R' - 1)}. \quad (5)$$

The differential area element is given by

$$dA = r^2 (R' + 1 - \cos(u)) du dv \quad (6)$$

Letting  $C'_0 = C_0 r$  and substituting into equation 2 gives

$$E_b = K_b \int_0^{\frac{\pi}{2}} \int_0^{2\pi} \left( -\frac{2 \cos(u) - R' - 1}{2(\cos(u) - R' - 1)} - C'_0 \right)^2 (R' + 1 - \cos(u)) du dv \quad (7)$$

which is scale invariant and the guassian term in eq. 2 has been omitted, as it is constant for the constant topology of the model crista junction. Carrying out the indicated integrations yields

$$E_b = 2K_b \pi \left( \frac{(R' + 1)^2}{\sqrt{R'^2 + 2R'}} \tan^{-1} \left( \frac{\sqrt{R'^2 + 2R'}}{R'} \right) - \left( \frac{C'_0}{2} + 1 \right) \left( 2 - \pi \frac{C'_0}{2} \left( R' + 1 - \frac{2}{\pi} \right) \right) \right) \quad (8)$$

for the energy of the model crista junction as a function of the reduced radius  $R'$  and spontaneous curvature  $C'_0$ . Entities that are distributed around an energetic minimum have an exponential distribution derived by Boltzmann. In what follows we will compare the observed distribution of  $R'$  with the Boltzmann distribution based on this energy. To that end we compute

$$P(R') = \frac{e^{-\frac{E_b(R', C'_0)}{kT}}}{\int_0^{\infty} e^{-\frac{E_b(x, C'_0)}{kT}} dx} \quad (9)$$

the fraction of configurations with a particular value of  $R'$  according to a Boltzmann distribution neglecting degeneracy's. Equation 9 is similar in form to equation 1 in the asymptotic limit as  $R'$  approaches 0 or  $\infty$ . Taking those limits in equation 8 gives

$$\left\{ \begin{array}{ll} E_b = \frac{K_b \pi^2}{\sqrt{2R'}} & R' \rightarrow 0 \\ E_b = \frac{K_b \pi^2 R'}{2} (C'_0 + 1)^2 & R' \rightarrow \infty \end{array} \right\}. \quad (10)$$

Identifying these two forms with the two terms in equation 1 enables us to use the best fitting values of  $a$  and  $b$  in that form to calculate the quantities  $K_b$  and  $C'_0$ .

To find the most probable value  $\bar{R}'$  of  $R'$  in the distribution in equation 9, we minimize  $E_b$  obtaining the condition

$$C'_0 = \left( \frac{1}{\sqrt{\pi}} \sqrt{\pi + \frac{2(R'+1)}{R'(R'+2)}} - \frac{4(R'+1)(R'^2 + 2R' - 1) \tan^{-1} \left( \frac{\sqrt{R'(R'+2)}}{R'} \right)}{(\sqrt{R'(R'+2)})^3} - 1 \right) \quad (11)$$

from which the value of  $\bar{R}'$  can be calculated.

## RESULTS

*The homogeneity of crista junctions is not preserved when measuring shape ( $R'$ ) as opposed to diameter.*

Evaluation of equation 2 for the geometry of a model crista junction showed that the shape of the junction rather than the size of the junction determined the bending

energy. To test this conclusion, measurements of  $R'$  were made on a subset of mitochondria from three different sources. Strikingly, the homology that existed in the measurements of crista junction diameters did not exist for the measurements of  $R'$ . ANOVA tests on the  $R'$  values suggested that the measurements segregated into two groups. Crista junctions from chick cerebellum and rat striatum were similar and were significantly different from crista junctions from mouse retina (figure 2). This variation in  $R'$  was directly attributable to  $r$ , as the average radii  $R$  of the three mitochondrial types were again statistically equivalent. (Figure2)

*Curve fitting of the distributions of  $R$  and  $R'$  show that Boltzmann distributions model the data better than does a normal distribution*

Measurements of  $R'$  were pooled into two groups described above and their distributions were fit both by equation 9 and by a normal distribution using the least-squares method (figure 2). A normal distribution would suggest that the crista junctions are randomly distributed about a mean versus the energetic distribution predicted by equation 9. Chi-squared values were then calculated to determine goodness of fit. By inspection, the Boltzmann fit better follows the sharp rise on the left of the peaks and the tail on the right. This impression is confirmed by the better chi-squared values (Table 1). The resulting parameters  $C_0$  and  $K_b$  explain the break in homology. The difference in average  $R'$  is due to the difference in spontaneous curvature ( $C_0$ ) whereas the bending modulus ( $K_b$ ) of the two groups appear to be nearly equal. Using the fitted form of equation 9, we calculated values of  $r$  from which the model crista junctions (Figure 3ab) could be drawn.

*Elliptical junctions are stable only for a specific range of spontaneous curvature and flare.*

We used our theoretical model to look for conditions where elliptical junctions would have bending energies comparable or less than circular junctions and thus be well represented in a Boltzmann distribution. Equations 3-7 were modified to model an elliptical junction. We looked for values of  $C_0$  and  $r$  at which the bending energy of an elliptical junction, with a major to minor axis ratio of 2, ( $R_1/R_2 = 2$ ) was less than that of a circular junction. For a junction with a radius  $R$  of 10nm, a circular junction has lower energy than the elliptical, ( $R_1=20\text{nm}$ ,  $R_2=10\text{nm}$ ) except when the flare becomes very large ( $R' < 1$ ). When the flare is larger than about 50nm, there exist a small range of spontaneous curvature values for which the elliptical junction has lower energy (Figure 3d). Within this range, for a given spontaneous curvature there should be a good representation of elliptical crista junctions with a major to minor axis ratio near 1.5 in the distribution of shapes. (Figure3e) Figure 3c shows the model for such a junction.

Comparison of elliptical junctions with  $R_1=10\text{nm}$ ,  $R_2=5\text{nm}$  or  $\sqrt{R_1^2 + R_2^2} = 10\text{nm}$  with the same circular junction yielded the same type of qualitative results. This explains slot like junctions seen in *N.Crassa* mitochondria. When  $C_0 = 1/2r = C_2/2$ , straight segments, were  $R \rightarrow \infty$  thus  $C_1 \rightarrow 0$ , result in equation 2 becoming zero. Thus in this region elongation of the major axis would involve minimal amounts of energy.

*Creation of a crista junction requires an outer-membrane.*

In another approach we used the program Surface Evolver to calculate a surface that fluctuates around the minimum of the bending energy. Starting with a sphere (figure

4a) we attempted to create a crista by increasing the surface area while constraining the volume. This resulted only in shapes that are simple deformations of a sphere. No shapes could be generated in this manner that resembled a crista. In mitochondria visualized *in situ* the volume is constrained by the surface of the outer membrane. To simulate this, a hard shell was put around the vesicle and the surface area was increased. This causes buckling of the membrane as its surface area becomes larger than the surface area of the containing shell (figure 4b). At some critical value of the surface area, one or two cristae are formed allowing the excess membrane to be directed into the lumen of the vesicle (Figure 4c). These cristae are light bulb shaped and are connected to the surrounding sphere via narrow necks. Elliptical junctions are observed in these simulations (figure 4d,e), but only as intermediates as the junction fluctuates around a circular cross-section. (Figure 4c). Detachment of the crista or other changes in the topology of the surface would give different shapes with lower energy (Julicher 1996; Seifert 1991). We neglect these events for two reasons; (1) we only see evidence of detached cristae in permeated mitochondria, though others have seen it under disease conditions (Mannella *et al* 2001), and (2) changes in topology, i.e. fission of crista, would occur after formation and enlargement of single crista. Our results show that bending energy alone is sufficient to lead to spontaneous crista formation in an encased membrane with sufficient surface area.

## **DISCUSSION**

The use of electron tomography to study the mitochondria in 3-dimensions has led to new ideas about the structure and function of the mitochondria (Mannella *et al* 2001; Mannella 2000; Perkins and Frey 2000; Frey and Mannella 2000). First, electron tomography allowed for the recognition of the crista junction (Perkins *et al* 1997;

Mannella *et al* 1994). Later, the existence of a new class of contact sites between the inner and outer membranes was discovered. (Perkins *et al* 2001). Now, we have proposed how an existing theoretical model: (1) Explains an architectural motif of the mitochondrion and (2) Provides insight into the possible mechanical properties of the inner membrane. Using the theory of spontaneous curvature to model the crista junction we find that the observed distribution of crista junction shapes matches a Boltzmann distribution for the bending energy. Analyzing shape ( $R'$ ) instead of size ( $R$ ) revealed differences in crista junctions that were previously thought to be uniform.

The fact that the distribution of bending energies in crista junctions fits very well to a Boltzmann distribution is reasonable. The total energy of the surface is additive and barring other constraints each degree of freedom would be expected to be close to its stationary distribution. This should apply also the value of  $C_0$  which reflects differing lipid composition and / or differing composition of membrane-bound and membrane-associated proteins. A mechanism, whereby  $C_0$  changes to accommodate the local curvature in accordance with equation 11, is not hard to imagine. This scenario is discussed by (Goetz and Gompper 1998) and suggested by figure 3 in that the model shapes of crista junctions found are distributed near the global minimum of the shape.

The tendency of lipid monolayers to curve is quantified by the monolayer's intrinsic radius of curvature,  $R_0$ , which is positive for most naturally occurring lipids indicating a tendency to curve toward the hydrophilic surface. A bilayer that is symmetric in lipid composition and concentration would have two monolayer leaflets with equal but opposite tendencies to curve and would, therefore, have a spontaneous curvature,  $C_0 = 0$ . A lipid bilayer can, however, have a nonzero  $C_0$  if the two leaflets

have different compositions. It is not known whether the two leaflets of the inner mitochondrial membrane have different compositions, but the inner membrane does contain high concentrations of phosphatidyl ethanolamine, a so-called nonbilayer lipid, and of phosphatidyl choline, a bilayer lipid. Nonbilayer lipids are also called polymorphic lipids as they tend to form the hexagonal  $H_{11}$  phase when purified and hydrated and have small  $R_0$ 's (ca. 2-3 nm for dioleoyl phosphatidyl ethanolamine), while bilayer lipids form bilayers under the same conditions and have larger  $R_0$ 's (ca 7-8 nm for dioleoyl phosphatidyl choline) (Streicher-Scott *et al* 1994; Gruner 1985). Nonbilayer lipids have been proposed as playing a role in facilitating membrane fusion and exocytosis (Gruner 1985) and there is evidence that they promote optimal activity of some membrane proteins (Streicher-Scott *et al* 1994). We suggest that they also facilitate the formation of complex membrane topologies as found in the inner mitochondrial membrane that must support sharp bends at crista junctions. The energy required to bend the membrane in crista junctions could be relaxed to a significant extent if nonbilayer phospholipids with smaller  $R_0$ 's migrated to the inside leaflet at crista junction curves and bilayer lipids with larger  $R_0$ 's migrated to the outside leaflet generating a lipid bilayer with a nonzero spontaneous curvature,  $C_0$ .

Finally, we examine the conditions that effect  $r$  and  $R$ . The excellent fit of observed shapes to a Boltzmann distribution peaked at the minimum of the bending energy for crista junctions suggests that a similar approach might qualitatively explain much more concerning the observed morphologies. We would suggest the following model free energy function for a crista

$$F = \frac{\pi K_b l}{R} + 2\pi P l R^2 + \pi K_b l C_0^2 R - 2\pi K_b l C_0 \quad (12)$$

which results from equation 3 for a cylinder with length  $l$ , radius  $R$ , osmotic pressure  $P$ , and assuming no stretching of the lipid bilayer. This model free energy relates the radius of the crista junction to the volume of the matrix. When the matrix contracts due to changing osmotic pressure, the contribution of  $R^2$  becomes smaller and when the matrix expands the contribution becomes greater. This results in a smaller average  $R$  when the matrix expands and a larger average  $R$  when the matrix contracts in agreement with figure 2b.

Previously, we asserted that crista grow from tubes and then merge with other cristae in the matrix to form lamellar structures (Perkins *et al* 2001). Figure 4 illustrates that this proposal can be at least qualitatively accounted for entirely by the theory of bending energies. The addition of membrane to the inner membrane results in areas of buckling that relax to form a tubular invagination. As more membrane is added buckling again occurs, but the membrane can relax by the diffusion of lipids to existing crista causing them to elongate. New cristae are formed when added lipids cannot diffuse fast enough to existing cristae. The local buckling then relaxes by growing a new crista.

We suggest that in the formation of a new junction and crista, the spontaneous curvature is zero or near zero and the initial flare is on the order of 20nm. The flare is under pressure from the volume of the matrix to become smaller. In doing so either the energy in the junction increases or the spontaneous curvature can increase in accordance with equation 11. The energy of the junction can keep decreasing with  $r$  becoming

smaller and  $C_0$  increasing until the global minimum is reached or  $C_0$  becomes limited by the properties of the membrane.

The variation of crista junction radii has real implications for the function of mitochondria. First if the earlier hypothesis (Mannella *et al* 2001) that the crista junctions act as a barrier to diffusion is correct, then, linking the size and the shape of the crista junction to matrix volume provides mitochondria with a mechanism by which they can regulate the size of this barrier. If crista junctions are an effective barrier to the diffusion of cytochrome c, then its full release during apoptosis must be accompanied by a reduction of matrix volume. This would run counter to proposals that matrix swelling leads to cytochrome c release (Green and Reed 1998), but consistent with observations of crista remodeling (Scorrano *et al* 2002). Thus the spontaneous curvature theory applied to mitochondria has implication for its function as well as its structure.

#### ACKNOWLEDGEMENTS:

T. G. Frey acknowledges support from Grant-in-Aid #0050769Y from the Western States Affiliate of the American Heart Association. C.W. Renken was supported by NIH/NIGMS MBRS program grant 1R25 GM58906. This work was supported in part by the National Institutes of Health, National Center for Research Resources Grant RR04050 to M. H. Ellisman.

## Reference List

Brakke M. (1992). The surface evolver. *Exp. Math* **1**(2):141-65.

Canham PB. (1970). The minimum energy of bending as a possible explanation of the biconcave shape of the human red blood cell. *J. Theor. Biol.* **26**(1):61-81.

Daems WT, Wisse E. (1966). Shape and attachment of the cristae mitochondriales in mouse hepatic cell mitochondria. *J. Ultrastruct. Res.* **16**(1):123-40.

Frey TG, Mannella CA. (2000). The internal structure of mitochondria. *Trends Biochem. Sci.* **25**(7):319-24.

Gozdz WT, Gompper G. (1998). Composition-Driven Shape Transformations of Membranes of Complex Topology. *Phys. Rev. Lett.* **80**(19):4213-6.

Green DR, Reed JC. (1998). Mitochondria and apoptosis. *Science* **281**(5381):1309-12.

Gruner SM. (1985). Intrinsic curvature hypothesis for biomembrane lipid composition: a role for nonbilayer lipids. *Proc. Natl. Acad. Sci. U.S.A.* **82**(11):3665-9.

Hackenbrock CR. (1966). Ultrastructural bases for metabolically linked mechanical activity in mitochondria. I. Reversible ultrastructural changes with change in metabolic steady state in isolated liver mitochondria. *J. Cell Biol.* **30**(2):269-97.

Helfrich W. (1973). Elastic properties of lipid bilayers: theory and possible experiments. *Z. Naturforsch. [C]* **28**(11):693-703.

Hessler D, Young SJ, Carragher BO, Martone ME, Lamont S, Whittaker M, Milligan RA, Masliah E, Hinshaw JE, Ellisman MH. (1992). Programs for visualization in three-dimensional microscopy. *Neuroimage* **1**(1):55-67.

Jie Y, Quanhui L, Jixing L, Zhong-can OY. (1998). Numerical observation of nonaxisymmetric vesicles in fluid membranes. *Phys. Rev. E* **58**(4):4730-6.

Julicher F. (1996). The morphology of vesicles of higher topological genus: Conformal degeneracy and conformal modes. *J. Phys. II* **6**(12):1797-824.

Jung HT, Coldren B, Zasadzinski JA, Lampietro DJ, Kaler EW. (2001). The origins of stability of spontaneous vesicles. *Proc. Natl. Acad. Sci. U.S.A.* **98**(4):1352-7.

Kluck RM, Esposti MD, Perkins G, Renken C, Kuwana T, Bossy-Wetzels E, Goldberg M, Allen T, Barber MJ, Green DR, and others. (1999). The pro-apoptotic proteins, Bid and Bax, cause a limited permeabilization of the mitochondrial outer membrane that is enhanced by cytosol. *J. Cell Biol.* **147**(4):809-22.

Lipowsky R. (1991). The conformation of membranes. *Nature* **349**(6309):475-81.

Lutter M, Perkins GA, Wang X. (2002). The pro-apoptotic Bcl-2 family member tBid localizes to mitochondrial contact sites. *BMC Cell Biol.* **2**(1):22

Mannella CA. (2000). Introduction: our changing views of mitochondria. *J. Bioenerg. Biomembr.* **32**(1):1-4.

Mannella CA, Marko M, Penczek P, Barnard D, Frank J. (1994). The internal compartmentation of rat-liver mitochondria: tomographic study using the high-voltage transmission electron microscope. *Microsc. Res. Tech.* **27**(4):278-83.

Mannella CA, Pfeiffer DR, Bradshaw PC, Moraru II, Slepchenko B, Loew LM, Hsieh CE, Buttle K, Marko M. (2001). Topology of the mitochondrial inner membrane: dynamics and bioenergetic implications. *IUBMB Life* **52**(3-5):93-100.

Naito H, Okuda M, Zhong-can OY. (1995). New solutions to the Helfrich variation problem for the shapes of lipid bilayer vesicles: Beyond Delaunay's surfaces. *Phys. Rev. Lett.* **74** (21):4345-8.

Perkins G, Renken C, Martone ME, Young SJ, Ellisman M, Frey T. (1997). Electron tomography of neuronal mitochondria: three-dimensional structure and organization of cristae and membrane contacts. *J. Struct. Biol.* **119**(3):260-72.

Perkins GA, Frey TG. (2000). Recent structural insight into mitochondria gained by microscopy. *Micron* **31**(1):97-111.

Perkins GA, Renken CW, Frey TG, Ellisman MH. (2001). Membrane architecture of mitochondria in neurons of the central nervous system. *J. Neurosci. Res.* **66**(5):857-65.

Perkins GA, Renken CW, Song JY, Frey TG, Young SJ, Lamont S, Martone ME, Lindsey S, Ellisman MH. (1997). Electron tomography of large, multicomponent biological structures. *J. Struct. Biol.* **120**(3):219-27.

Perkins GA, Song JY, Tarsa L, Deerinck TJ, Ellisman MH, Frey TG. (1998). Electron tomography of mitochondria from brown adipocytes reveals crista junctions. *J. Bioenerg. Biomembr.* **30**(5):431-42.

Scorrano L, Ashiya M, Buttle K, Weiler S, Oakes SA, Mannella CA, Korsmeyer SJ. (2002). A distinct pathway remodels mitochondrial cristae and mobilizes cytochrome c during apoptosis. *Dev. Cell.* **2**(1):55-67.

Seifert U. (1991). Vesicles of Toroidal Topology. *Phys. Rev. Lett.* **66**(18):2404-7.

Streicher-Scott J, Lapidus R, Sokolove PM. (1994). The reconstituted mitochondrial adenine nucleotide translocator: effects of lipid polymorphism. *Arch. Biochem. Biophys.* **315**(2):548-54.

von Ahsen O, Renken C, Perkins G, Kluck RM, Bossy-Wetzel E, Newmeyer DD. (2000). Preservation of mitochondrial structure and function after Bid- or Bax-mediated cytochrome c release. *J. Cell Biol.* **150**(5):1027-36.

Zhong-can OY, Helfrich W. (1987). Instability and deformation of a spherical vesicle by pressure. *Phys. Rev. Lett.* **59**(21):2486-8.

Zhong-can OY, Helfrich W. (1989). Bending energy of vesicle membranes: General expressions for the first, second, and third variation of the shape energy and applications to spheres and cylinders. *Phys. Rev. A* **39**(10):5280-8.

Zhou J, Zhang Y, Zhou X, Zhong-Can O. (2002). Large deformation of spherical vesicle studied by perturbation theory and surface evolver. *Int. J. Mod. Phys. B* **15**(22):2977-91.

## Figure Captions

Figure 1. A-C. Surface rendered mitochondria from electron tomograms show the nature of crista junctions, outlined in red. A. Mitochondria *in situ* from Chick Cerebellum. B. Isolated Xenopus egg mitochondria. C. Isolated Xenopus egg mitochondria after permeation of the inner membrane. D. Model crista junction showing the two radii of curvature that define its shape.

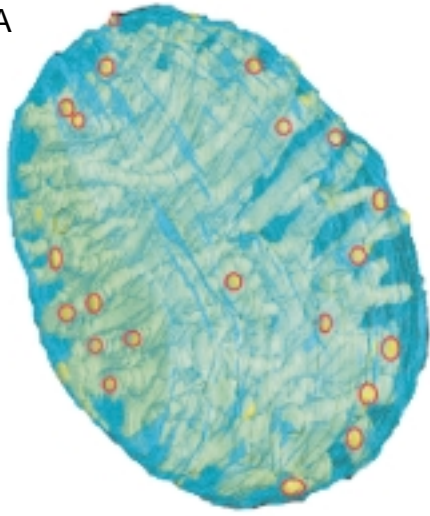
Figure 2. Analysis of crista junction parameters measured from tomograms from indicated sources. A. Average radii of crista junctions for six types of *in situ* mitochondria. B. Average radii of crista junctions from Isolated Xenopus egg mitochondria in the condensed and permeated states. C. Average ratio of radii ( $R'$ ) for three types of mitochondria. D-E. Distribution of crista junction parameters from *in situ* mitochondria fit to an exponential distribution (solid line) and normal distribution (dashed line). D. Distribution of crista junction radii from all mitochondrial types. E. Distribution of  $R'$  for crista junctions from Mouse Retina. F. Distribution of  $R'$  for crista junctions from Chick Cerebellum and Rat Striatum. \* Indicates significance of  $P < .001$  by student t-test.

Figure 3. Crista junction shape and energy. A, B and E model crista junctions with a radius of 10nm. A. Shape of crista junction that approximates the crista junction in Mouse Retina with  $r = 8$  nm. B Shape of crista junction in Rat Striatum and Chick Cerebellum with  $r = 12$  nm. E. Stable elliptical junction with  $R_1 = 15$  nm,  $R_2 = 10$  nm and  $r =$

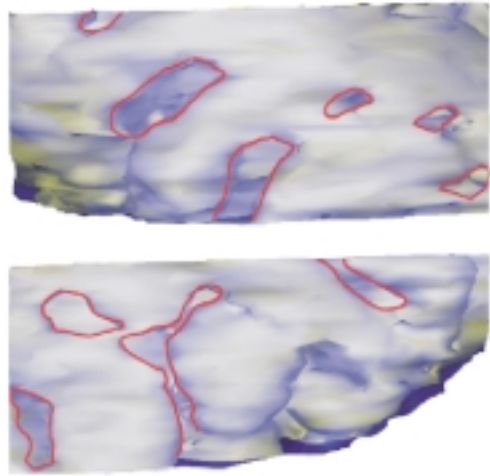
80nm. C. Energy contours of crista junctions with a radius of 10nm and the indicated  $r$  and  $C_0$ . Solid purple area with lower case  $e$  in bottom left hand corner indicates the region where an elliptical junction with  $R_1=20\text{nm}$ ,  $R_2=10\text{nm}$  has less energy than a circular junction of  $R = 10\text{nm}$  for the given values of  $C_0$  and  $r$ . Lower case letters mark the position of the respective crista junction. D. Energy contour of a crista junction with  $R_2 = 10 \text{ nm}$ ,  $r = 80 \text{ nm}$ , and the indicated  $R_1$  and  $C_0$ .

Figure 4. Shapes generated by Surface Evolver under the following conditions. A. Initial sphere. B Membrane enclosed in hard shell and volume maximized while surface area is increased. C. Same conditions as B after the addition of more surface area. D, E and F. Transient elliptical junction created under conditions of C.

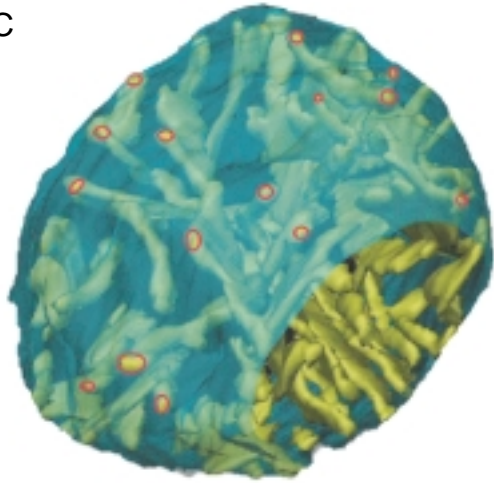
A



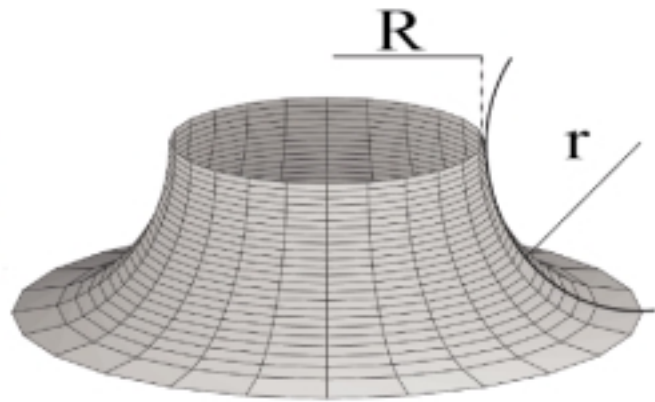
B

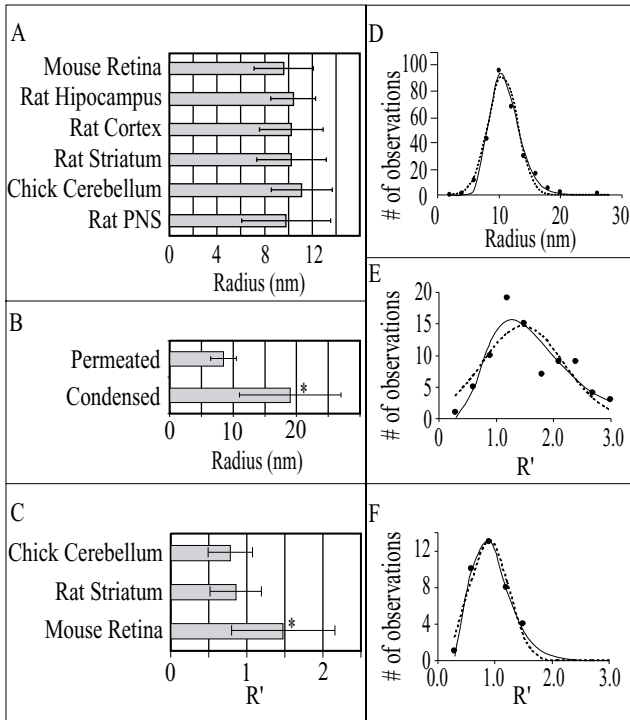


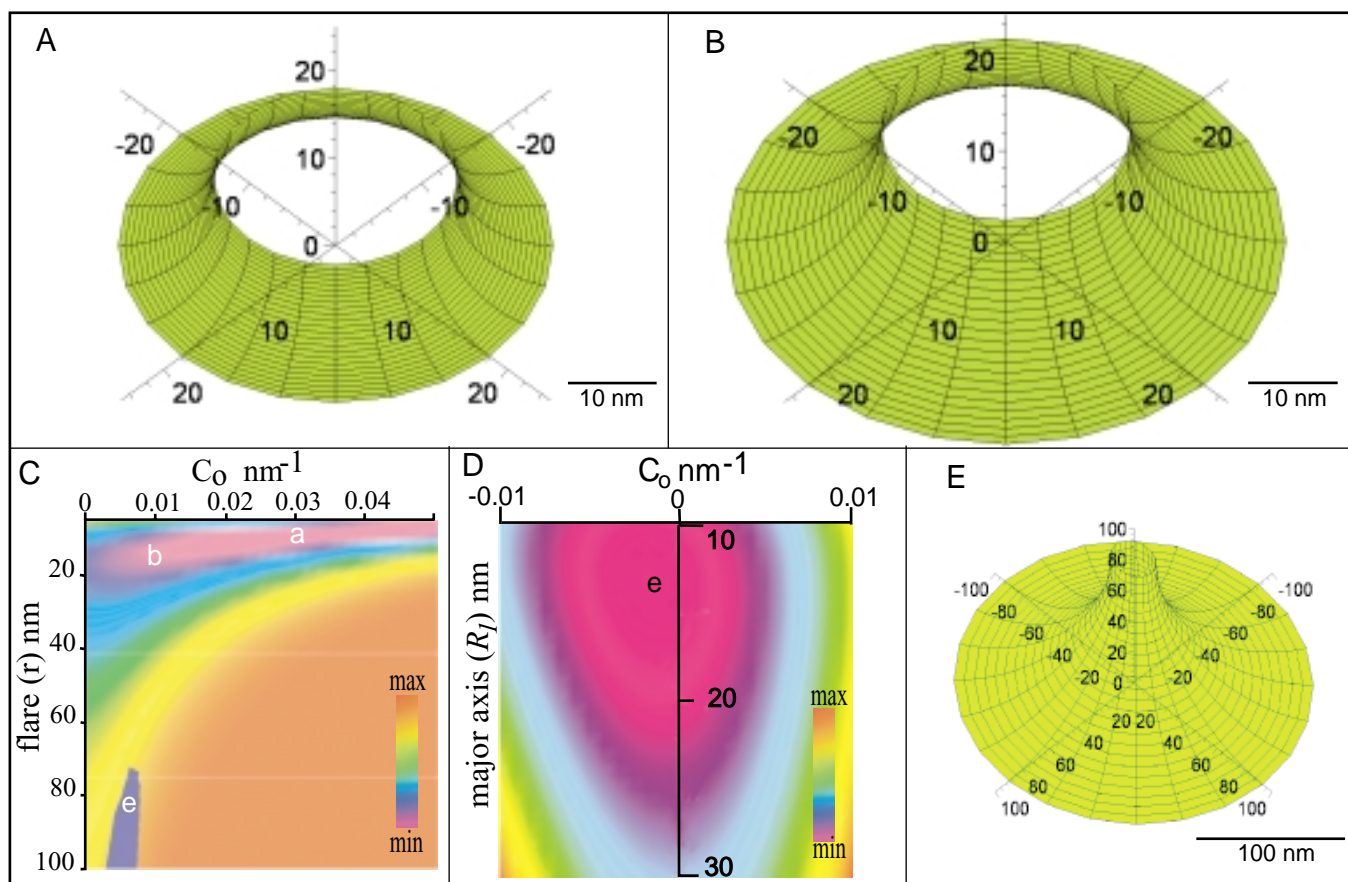
C



D







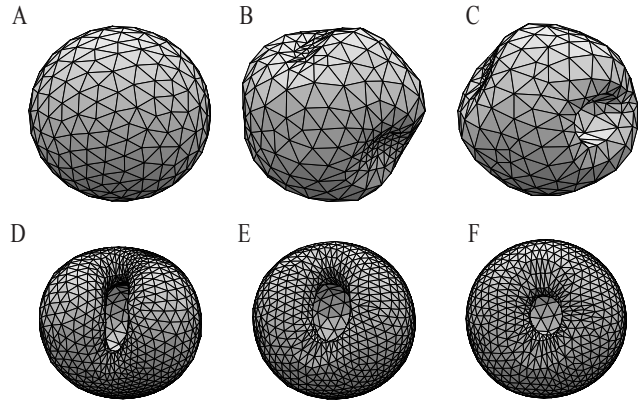


TABLE I  
Goodness of fit and related parameters from distribution of crista junction shapes ( $R'$ )

Distribution	Parameters	Mitochondrial type	
		<i>Mouse Retinal</i>	<i>Rat Striatum Chick Cerebellm</i>
Normal Distribution	$\chi^2$	11.8	2.1
	Ave $R'$	$1.5 \pm 0.7$	$0.9 \pm 0.3$ §
	r	7nm	11nm
Exponential Distribution	$\chi^2$	8.5	0.8
	$\bar{R}'$	1.29	0.81
	r	7.8 nm	12.3 nm
	Co	$0.0316 \text{ nm}^{-1}$	$0.0097 \text{ nm}^{-1}$
	$K_b$	2.8kT	3.4kT
	$E(\bar{R}')$	0.9kT	2.0kT

§ Significant difference from *Mouse Retinal* by student t-test  $P < 0.005$

$\bar{R}'$  is the  $R'$  value with the highest probability

$E(\bar{R}')$  is the energy in a crista junction of  $R' = \bar{R}'$